Analysis of Transport Mechanism of Binary Organic Solvent System through a PDMS-based Dense Membrane Using a Regular Solution Model Combined with a Solution Diffusion Model

Atsushi Miyagi, [a]* Hiroshi Nabetani,[b] and Mitsutoshi Nakajima[c]

[a]Chiba Industrial Technology Research Institute, 889 Kasoricho, Wakabaku, Chiba 264-0017, Japan

[b]National Food Research Institute, National Agriculture and Food Research Organization, Tsukuba, Ibaraki 305-8642, Japan

[c]Graduate School of Life and Environmental Sciences, University of Tsukuba, Tsukuba, Ibaraki 305-8572, Japan

Correspondence:

Atsushi Miyagi, Chiba Industrial Technology Research Institute, 889 Kasoricho, Wakabaku, Chiba 264-0017, Japan

Tel: +81-43-231-4346 Fax: +81-43-233-4861

E-mail: a.myg@pref.chiba.lg.jp

ABSTRACT: In the present study, transport mechanisms of various binary systems such as alcohol-hexane, alkane-hexane, lipid-hexane, and diesel fuel-kerosene systems through a PDMS-based dense membrane were investigated using a combined regular solution (RS) and solution-diffusion (SD) model at constant pressure and temperature. The combined model contains many important factors for permeability such as diffusivity, degree of swelling membrane, membrane thickness, and osmotic pressure. Total, hexane, and solvent fluxes (except for a part of the solvent flux) of all systems were controlled by molar volumes of hexane and solvent and solubility parameters of hexane, solvent, and membrane polymer based on the combined model. The selectivity of the solvent in these systems seems to depend upon the similarity of the molecular structures of hexane and solvent, corresponding to entropy mixing, and the interaction of the hexane-solvent-membrane polymer, corresponding to enthalpy mixing. The combined model could well describe the transport mechanism of the binary system.

KEY WORDS: binary system, combined model, permeability, PDMS-based dense membrane, regular solution model, selectivity, solution-diffusion model

1 1. Introduction

2 The membrane process is remarkably simple, offering many advantages over
3 other separation processes (e.g., distillation). These advantages include low energy
4 consumption, ambient temperature operation, and retention of nutrients. Therefore,
5 this process has been applied mainly to aqueous systems in various industries.
6 Recently, many researchers have attempted to apply membrane technology to
7 non-aqueous systems, due to the development of a solvent-resistant membrane. In
8 particular, a dense nonporous membrane has been widely applied to gas separation
9 [1-3], pervaporation [4, 5], and nanofiltration [6, 7]. We also employed a
10 PDMS-based dense membrane for purifying crude vegetable oil [8, 9], used frying
11 oil [10, 11], fish oil [12], and crude fatty acids [13]. We propose that membrane
12 technology has the potential to become an alternate process in the oil and fat
13 industry. In the wake of membrane technology's spreading to non-aqueous
14 applications in the oil, fat, and petroleum industries, clarification of the membrane
15 transport mechanism is important.

16 Many studies have used the solution-diffusion (SD) model to analyze the
17 transport mechanism in dense nonporous membranes [14-20]. For example, Stafie
18 *et al*. [16] investigated the transport of hexane-solute systems through a
19 tailor-made composite (NF) membrane and reported that the SD model offers a
20 reasonably accurate description of the aspects of hexane transport in these systems.
21 Han *et al.* [17] studied the transport of toluene through organic solvent silicone
22 rubber membranes and observed that the solute-membrane interaction provides a
23 major contribution to the mass transport of toluene through the membrane. Thus,
24 the SD model may be appropriate for describing the transport of solvent through a

membrane [17]. The Subramanian group [18-20] applied the SD model using a PDMS-based composite membrane by investigating the separation mechanism of oil constituents such as triglyceride-oleic acid, triglyceride-tochopherol, and vegetable oil-hexane systems. In the triglyceride-oleic acid system, the preferential permeation of oleic acid is due to preferential sorption and concentration-dependent solubility and diffusivity resulting from the interaction of the penetrants with the membrane [18]. In the triglyceride-tochopherol system, the tochopherol preferentially permeated the membrane and the total permeate flux tended to be constant, regardless of an increase in tochopherol concentration and feed viscosity [19]. This result indicates that the preferential sorption (solubility) of tochopherol may play a significant role in the permeation process [19]. An inverse relationship between viscosity or molecular weight and total flux was observed in the vegetable oil-hexane system [20]. These observations confirm that the transport mechanism follows the SD model.

In contrast, we first proposed a transport mechanism for a single organic solvent system through the PDMS-based dense membrane by using a regular solution (RS) model. We found that the permeate flux of solvent (J_s) demonstrated a linear dependency on the product of the molar volume of solvent (V_s) and the square of the difference in the solubility parameter between the membrane polymer and solvent ($(\delta_{mem} - \delta_s)^2$) at a constant pressure and temperature [21]. This approach was also in agreement with the results of an analysis based on the SD model [21].

In the present study, a model combining the RS model and the SD model is proposed for the first time. The permeability and separation performance of

various binary systems (e.g., alcohol-hexane, alkane-hexane, diesel fuel-kerosene, and lipid-hexane systems) using the PDMS-based dense membrane process were characterized, and the transport mechanism was analyzed with the combined model.

2. Theoretical background

2.1 Solution-diffusion (SD) model

This section summarizes the SD model, referring to the review reported by Hofmann et al. [22]. Membrane processes based on a SD mechanism are usually classified according to the states of the feed and permeate phases. The sorption of a penetrant molecule at the feed side is described by a solubility coefficient S, which correlates the pressure of the feed-side p_f, with the penetrant concentration of the feed-side C_f, in the uppermost layer of the polymer phase.

$$C_f = S\, p_f \tag{1}$$

Penetrants with higher solubility such as carbon dioxide and hydrocarbons often exhibit stronger interactions with each other and with the polymer matrix, resulting in swelling phenomena. This usually indicates a distinct concentration dependence of the S value

The diffusive transport across the membrane, represented by the flux J, is described by a diffusion coefficient D, and a concentration gradient (dC/dz), according to Fick's First Law.

$$J = - D \, (\mathrm{d}C/\mathrm{d}z) \qquad (2)$$

The desorption at the downstream (permeate side) interface (z = λ : membrane thickness) is described by a solution equilibrium using the pressure of the permeation-side p_p, and the concentration of permeation-side C_p.

$$C_p = S \, p_p \qquad (3)$$

When constant boundary conditions (p_f, p_p) are applied after a certain time, a steady state is reached and, assuming concentration-independent transport coefficients D and S, a linear concentration profile with a constant concentration gradient is established.

The flux in the steady state is

$$J = - D \, (C_p - C_f)/\lambda \, . \qquad (4)$$

Introducing the solubility coefficient one obtains

$$J = D \, S \, (p_f - p_p)/\lambda = D \, S \, \Delta p \, /\lambda \, . \qquad (5)$$

The concentration gradient leads to the production of an osmotic pressure, $\Delta\pi$, according to the van 't Hoff law.

$$\Delta\pi = (C_p - C_f) \, RT = \Delta C \, RT \qquad (6)$$

where, R is the gas constant and T is the temperature. The osmotic pressure definition is inserted into Eq. (5).

$$J = D\,S(\Delta p - \Delta\pi)/\lambda \tag{7}$$

2.2 Combining the regular solution (RS) model with the SD model.

In adopting the SD model, it is implicitly assumed that the rates of adsorption and desorption at the membrane interface far exceed the rate of diffusion through the membrane [14]. Therefore, accurate characterization of the solubility of a given solvent in a membrane polymer is very important.

In order to develop the solution model, the membrane interface of the feed-side was noted, and the binary solvents in the present case were assumed to be homogeneous solvents, for simplicity. If a polymer is in the amorphous form, such as the membrane polymer used in this study, the solvent molecules will dissolve in the polymer [23]. When the permeate flux is steady at constant pressure and temperature, it is reasonable to postulate that a pseudo-static solution of the (binary) solvent in the membrane polymer is formed, and that the solution is in equilibrium with the solvent phase (retentate), as depicted in Fig. 1. When membrane polymer components and (binary) solvent are mutually soluble at constant pressure and temperature, the following relation can be proposed based on the regular solution model [23]:

$$\ln a = \ln x + V_s\,\Phi_{mem}^{\,2}\,(\delta_{mem} - \delta_s)^2/RT = \ln x' + V_s\,\Phi'^{\,2}_{mem}\,(\delta_{mem} - \delta_s)^2/RT, \tag{8}$$

where a is the activity of the solvent in the membrane phase, x is the concentration (mole fraction) of the solvent in the membrane phase, V_s is the molar volume of solvent, Φ_{mem} is the volume fraction of membrane polymer in the membrane phase, x' is the mole fraction of solvent in the solvent (retentate) phase, δ_{mem} is a solubility parameter of the membrane polymer, δ_s is the solubility parameter of the solvent, and Φ'_{mem} is the volume fraction of the membrane polymer in the solvent phase. A smaller Φ_{mem} value corresponds to a larger volume fraction of solvent in the membrane phase ($1-\Phi_{mem}$); that is, Φ_{mem} indicates the degree of swelling.

Since the membrane polymer does not dissolve in the solvent, the solvent in the solvent phase can be regarded as pure solvent; specifically, $\Phi'_{mem} = 0$, and $x' = 1$. Consequently, Eq. (9) is derived from Eq. (8) as follows.

$$\ln a = \ln x + V_s \Phi_{mem}^2 (\delta_{mem} - \delta_s)^2 / RT = 0$$

$$\ln x = -V_s \Phi_{mem}^2 (\delta_{mem} - \delta_s)^2 / RT \quad (9)$$

This equation indicates that with smaller values of Φ_{mem}^2, V_s, and $(\delta_{mem} - \delta_s)$ (i.e., when there is a larger degree of membrane swelling, a smaller solvent molecule, and less interaction intensity between solvent and membrane), a larger mole fraction of solvent exists in the membrane, and vice versa.

The RS model characterizes the solubility, which is the S value in Eq. (7) derived by the SD model. By combining Eq. (7) with Eq. (9) and replacing x/λ with S, the following equation is obtained:

$$J = (D\,(\Delta p - \Delta\pi)/\lambda^2)\,\exp\,[-\,(\Phi_{mem}{}^2\,V_s\;(\delta_{mem} - \delta_s)\,/RT)] \qquad (10)$$

that is, the combination of the RS model with the SD model is expressed in this equation.

2.3 Parallelism of chemical potential between SD and RS models.

The starting point for the mathematical description of permeation in all membranes is the proposition, solidly based in thermodynamics, that the driving forces of pressure, temperature, concentration, and electromotive force are interrelated and that the overall driving force producing movement of a permeate is the gradient in its chemical potential [14]. The flux J, can be described by a simple equation using the gradient in chemical potential ($d\mu/dz$), as in [14]:

$$J = -\,L\,(d\mu/dz) \qquad (11)$$

where L is a coefficient of proportionality linking the chemical potential driving force with the flux. Since temperature is maintained constant and the electromotive force can be considered negligible in the membrane process, the driving forces are restricted to concentration (activity) a, and pressure gradients in the chemical potential μ, are written as [14]:

$$d\mu = RT\,d(\ln(a)) + V dp \qquad (12)$$

The SD and RS models differ in the handling of the chemical potential gradient in the membrane phase. The SD model assumes that the pressure within a membrane is uniform and that the chemical potential gradient across the membrane is expressed only as a concentration gradient [14], while in the RS model, the equilibrium of the feed phase and the membrane phase on the membrane interface is characterized, so both phases should be regarded as in a homogeneous state with each other as a prerequisite. Thus, the RS model assumes that the concentrations of binary compounds within a membrane are uniform and that the chemical potential gradient across the membrane is expressed as a pressure gradient. This assumption is also adopted in the pore-flow model [14]. By combining the RS model with the SD model, the driving force can be represented by the pressure and concentration gradients.

2.4 Solubility parameter.

When adopting the SD model and/or RS model, the solubility parameter is an important concept for estimating the solubility. The solubility parameter δ, can be defined as [23, 24]

$$\delta = [(\Delta H - RT) / V]^{1/2} \tag{13}$$

where ΔH is the heat of vaporization.

In general, the solubility parameter is considered as being made up of various components, that is,

$$\delta^2 = \delta_d^2 + \delta_p^2 + \delta_h^2 \quad (14)$$

where δ_d, δ_p and δ_h are contributions due to dispersion forces, dipole-dipole interactions, and hydrogen bonding [23, 24]. However, since the regular solution equation is derived on the basis of a counterbalance between the entropy and energy of mixing without any specific interaction [23], in the present study, the solubility parameter difference of each solvent and the membrane was obtained by simply subtracting the literature values or calculated values.

3. Experimental

3.1 Reagents and membrane material

All alkane, alcohol, and lipids used were of reagent grade and purchased from Wako Pure Chemical Industry. Kerosene and diesel fuel were procured from a gas station (Idemitzu Corp.) in Miyako-cho, Chiba, Japan.

The membrane used was a flat-sheet membrane (NTGS-2200, Nitto Denko Corporation) of the type used in commercial spiral wound modules and employed for gas separation applications (recovery of hexane vapors) in the petroleum industry. This membrane was prepared by casting 3μm-thick silicone (PDMS) polymer film onto a support layer (solvent-resistant porous polyimide) using a Gardner casting knife. A sectional view of the membrane produced using scanning electron microscopy was presented in our previous study [13]. The cross-linking degree of the skin layer (PDMS) is not clear.

Table 1 lists the molar volume V, and the molecular weight M, of these solvents and the solubility parameter δ, of the membrane, hexane, and solvent as

provided by the literature [13, 21].

3.2 Membrane apparatus

An apparatus with a magnetically stirred membrane cell (Model C-70B; Nitto Denko Corp.) used in the experiment was the same as in the previous reports [13, 21]. In all of the experiment runs, the temperature was 25^{o}C, the operating pressure was 1 MPa, and the speed of the spin bar was 200 rpm.

3.3 Binary systems

Experiments were conducted with eight binary solvent-hexane systems such as alcohol-hexane (alcohol: ethanol, 1-butanol, and 1-hexanol), alkane-hexane (alkane: decane, tridecane, and hexadecane) and lipid-hexane (lipids: oleic acid and triolein) systems, and with diesel-fuel-kerosene system.

3.4 Experiment methods.

Time courses of total permeate flux were determined for each system, and the stabilities were determined. The cell was initially charged with 100 g of 50/50 (g-solvent/g-hexane)or (g-diesel fuel/g-kerosene) feed samples, and the permeate was weighed periodically.

The total (weight) permeate flux J_T kg/(m^2 h) was calculated as follows:

$$J_T = W / (A\, t), \tag{15}$$

where W is the amount of the permeate (kg), A is the effective membrane area

(0.0032m^2), and t is the permeation time (h).

Separation performance for each system was determined as 50 g of solvent-hexane (or diesel fuel-kerosene) feed samples for 0/50, 10/40, 20/30, 30/20, 40/10, and 50/0 (g-solvent/g-hexane) or (g-diesel fuel/g-kerosene) was initially charged in the cell. The experiments were stopped when the permeates reached 5 g. The total, hexane and solvent fluxes and the composition of the feeds and permeates were determined.

3.5 Analysis

The composition of all solvent-hexane systems except the oleic acid-hexane and triolein-hexane systems, and of the diesel fuel-kerosene system, were determined using packed gas chromatography (GC 9A, Shimazu Corp.), injecting a 2 μL undiluted sample for the alkane-hexane and alcohol-hexane systems, or a 2 μL sample diluted with n-pentane by five times for the diesel-fuel-kerosene system. The operating conditions of these systems are summarized in Table 2. The packing materials used were polystyrene, polyethylene glycol, and silicone-based particles, which correspond to the Gascuropack 54, PEG-20 M, and Silicone SE-30 products, respectively (GL Sciences, Tokyo) (Table 2). The carrier gas was nitrogen, and the detector was FID (Table 2). A constant-temperature or programmed-temperature method was adopted, depending upon the binary system (Table 2).

The composition of the oleic acid-hexane and triolein-hexane systems was measured as follows. After the samples were weighed, the hexane was removed using a rotary flash evaporator, with any remaining traces removed by holding the

residues in a desiccator for 4h at 40°C under a vacuum (<5mm Hg of absolute pressure). The hexane-free residues were weighed to measure the amount of oleic acids or triolein.

3.7 Calculations

The mean molar volume V_m, the mean molecular weight M_m, and the mean solubility parameter δ_m, [25] of the permeate in all systems are defined as

$$V_m = \Sigma (y_i V_i) \quad (16)$$

$$M_m = \Sigma (y_i M_i) \quad (17)$$

$$\delta_m = \Sigma (y_i V_i \delta_i)/\Sigma (y_i V_i) \quad (18)$$

where y_i is the mole fraction of component *i* permeate, V_i is the molar volume of component *i*, M_i is the molecular weight of component *i*, and δ_i is the solubility parameter of component *i*.

The percentage rejection *PR* (%) of solvent, which is the common term for the selectivity in the membrane, was defined as

$$PR = 100 (1 - (Y/X)) \quad (19)$$

where *X* is the weight fraction of solvent in the feed and *Y* is that in the permeate.

When there were no data in the literature [13, 21] for the solubility parameter δ,

such as n-paraffin containing diesel fuel or kerosene, the group contribution method for predicting the solubility parameter was adopted. The following formula is given by [26]:

$$\delta = (\Sigma E_{coh} / \Sigma V_g)^{1/2} \quad (20)$$

where E_{coh} is the internal energy and V_g is the molar volume for each structural group. The value was calculated using the group contribution value of E_{coh} and V_g as listed in Table 3 [24].

4. Results

4.1 Total permeate flux

The total permeate flux *vs*. the total amount of permeate for all systems is presented in Fig. 3. Overall, the order of total permeate flux is alkane-hexane, alcohol-hexane, diesel fuel-kerosene, and lipid-hexane systems. In the alkane-hexane systems, the order of total permeate flux is decane-hexane, tridecane-hexane, and hexadecane-hexane systems, which is the inverse of the *V* or *M* value of alkane. In the alcohol-hexane systems, the total permeate fluxes are almost the same, in spite of the difference in the *V* or *M* value of the individual alcohol. In the lipid-hexane systems, the total permeate flux of oleic acid-hexane system is higher than that of in the triolein-hexane system, corresponding to the smaller *V* or *M* value of the lipids.

The percentage decrease *PD*, of total flux when the total amount of permeate reached 30g, J_{30}, compared with the initial total flux, J_0, is calculated as

$$PD = (J_{30} - J_0) / J_0 \times 100. \quad (21)$$

The *PD* of the alkane-hexane and diesel-fuel-kerosene systems is 1.0 to 2.5%, while that of the alcohol-hexane systems is 5.5 to 11%, indicating a slight reduction during the membrane process. The *PD* of the oleic acid-hexane system is 19%, and that of the triolein-hexane system is 44%, indicating a remarkable decrease compared to the other systems.

4.2 Separation performance

Table 4 presents X and Y, the mean molar volume of permeate V_m, the difference between the solubility parameter of the membrane polymer and the mean solubility parameter of an individual system $|\delta_{mem} - \delta_m|$, the total permeate flux J_T, the permeation rates of solvent J_s, and hexane J_{hex}, and the *PR* values for all of the solvent-hexane systems.

In all systems, J_T and J_{hex} decrease with an increase in X or Y. In the alkane-hexane systems, X and Y are approximately the same the *PR* values turn out to be almost 0 (Table 4). In the alcohol-hexane and the lipid-hexane systems, the Y values are lower than the X values, corresponding to positive PR values (Table 4); that is, hexane is preferentially passed through the membrane over alcohol or lipids. The pronounced reduction in total flux of the alcohol-hexane and lipid-hexane systems compared to that of the alkane-hexane systems during the membrane process (Fig. 3) is due to the increased solvent concentration of the retentate during the membrane process. These tendencies are particularly remarkable in the

triolein-hexane system. In almost all hexane-diluted systems, an optimum X value that leads to maximum J_s is observed (Table 4).

Table 5 presents the composition of n-paraffin and V_m and J_T values for the diesel fuel-kerosene system. The solubility parameter of each n-paraffin $\delta_{n\text{-}p}$, calculated by Eq. (20), and the $|\delta_{mem} - \delta_{n\text{-}p}|$ values are also presented in Table 5. The distribution of n-paraffin in kerosene is C_8 - $C_{17,}$ and that in diesel fuel is C_8 - C_{26}, the $|\delta_{mem} - \delta_{n\text{-}p}|$ value of each n-paraffin is within 1.3 $(J/cm^3)^{1/2}$ (Table 5). The composition of n-paraffin in feed and permeate is similar in all diesel-fuel-kerosene systems (Table 5). As mentioned before, the almost constant total flux course of both the diesel-fuel-kerosene system and the alkane-hexane system (Fig. 3) is due to the almost constant composition of the retentate during the membrane process. However, the permeate flux decreases with an increase in the proportion of diesel fuel (i.e., an increase in V_m value) (Table 5).

From the above, in alkane-hexane and the diesel fuel-kerosene systems, since the *PR* values are constant and the total fluxes with the total amounts of permeate are approximately constant, they can be regarded as maintaining a static state during the processing. In contrast, in alcohol-hexane and the lipid-hexane systems, *PR* values changed with the composition and the total flux decreased over time. This is due to the change in composition of the retentate as the process proceeds. However, since the changes appeared very smooth and continuous (Fig. 3), this can be considered as a pseudo-static state. The scheme of this state will be presented as Fig. 1. These results indicate that the all binary systems can apply the RS model as well as the SD model.

5. Discussion

5.1 Application of the SD model

Many studies have proposed using the SD model to analyze the permeability of non-aqueous systems through a dense membrane [14-21]. Numerous reports indicate that the solubility corresponds to the difference in solubility parameters between membrane and solvent, $|\delta_{mem} - \delta_s|$ [4, 5, 21], and that the diffusivity corresponds to the viscosity or MW of the solvent [15, 16, 18-21]. In the present study, the investigation of the permeability of binary systems adopts the SD model using the $|\delta_{mem} - \delta_s|$ and the MW values.

5.1.1 Diffusivity

In alkane-hexane, lipid-hexane, and diesel fuel-kerosene systems, a smaller M_m value leads to larger J_T and J_{hex} values (Table 4). Thus, a solvent with a smaller MW (or viscosity) results in higher diffusion of the solvent into the membrane polymer. Similar results have been observed in previous studies [16, 20, 21]. The Subramanian group attempted to determine the influence of feed MW or viscosity on the total flux for many vegetable oils with various hexane dilutions, using the same type of membrane that we used. They reported that all of these oils exhibited an inverse relationship with a high correlation between viscosity or MW and total flux, both undiluted and at various levels of hexane-dilution [20]. Stafie *et al*. reported that the viscosity inside the membrane and the swelling of the membrane are the most critical factors affecting hexane permeability [16].

In contrast, in all alcohol-hexane systems except the hexanol-hexane system,

the J_T and J_{hex} values did not decrease with the M_m value (Table 4). In these systems, the permeability cannot be explained entirely by the diffusivity.

5.1.2 Solubility

Previous studies reported that gas permeability through a membrane polymer was affected by boiling or by the critical temperatures of the gases [1]. The solubility parameter may therefore be useful for predicting permeability, since the heat of vaporization depends on these temperatures [23].

Several reports have proposed that smaller differences between the solubility parameters of membrane and solvent $|\delta_{mem} - \delta_s|$ implied greater solubility of the solvent into the membrane polymer [4, 5, 21]. Machado *et al*. reported that the flux of pure or mixed solvents through silicone-based nanofiltration membranes was affected by the surface tension and viscosity of the solvents [15]. In many cases, the surface tension correlates well with the solubility parameter [23]. In the present study, when δ_s was replaced by δ_m for the binary systems (δ_m is the mean solubility parameter of solvent and hexane (diesel fuel and kerosene)), a tendency for the alcohol-hexane and lipid-hexane systems was noticed: J_T and J_{hex} were inversely related to $|\delta_{mem} - \delta_m|$. However, in the alkane-hexane systems, no relationship between J_T or J_{hex} and $|\delta_{mem} - \delta_m|$ was found because of a pronounced low point compared to the values for the alcohol-hexane systems.

Based on the above discussion, the permeabilities of their systems can be explained by the SD model, but there seem to be some limitations on systematic determination.

5.2 Application of the combined model

We attempted to apply a combined model (Eq. (10)) to the present systems, replacing V and δ_s with V_m and δ_m, because they can be regarded as pseudo-static.

5.2.1 Analysis of permeate flux using the combined model

(1) Total and hexane fluxes

In the alcohol-hexane systems, the plots of $\ln(J_T)$ and $\ln(J_{hex})$ vs. $- V_m(\delta_{mem} - \delta_m)^2/RT$ exhibit reasonably good linear relationships (Fig. 4). These highly correlated linear relationships indicate that J_T and J_{hex} in these binary systems increase mainly with a decrease in V_m and $(\delta_{mem} - \delta_m)^2$, justifying the principle of the transport mechanism of penetrant through a dense nonporous membrane, based on the combined model.

In the alkane-hexane, diesel-fuel-kerosene, and lipid-hexane systems, it can be assumed that $|\delta_{mem} - \delta_m|$ (or, $|\delta_{mem} - \delta_{n\text{-}p}|$) is constant, as with the systems reported in our previous study, since the differences in $|\delta_{mem} - \delta_m|$ (or, $|\delta_{mem} - \delta_{n\text{-}p}|$) for the alkanes and the lipids are very low (within 1.9 $(J/cm^3)^{1/2}$) compared to those for the alcohols (Tables 4 and 5) and considering the error involved in determining these solubility parameters [21]. The plots of $\ln(J_T)$, $\ln(J_{hex})$ vs. V_m/RT yield an approximately straight line for the alkane-hexane and diesel fuel-kerosene (only $\ln(J_T)$ vs. V_m/RT), as seen in Fig. 4. In particular, the relationship between $\ln(J_T)$ and V_m/RT for all alkane-hexane systems has an almost identical line; furthermore, the approximate line for the diesel fuel-kerosene system nearly agrees with that for the alkane-hexane systems (Fig. 4).

In the lipid-hexane systems, an approximately linear relationship exists

between $\ln(J_T)$ and V_m/RT for the oleic acid-hexane system but not for the triolein-hexane system depicted in Fig. 4. However, by removing the data for undiluted triolein, the approximate line for the triolein-hexane system can be perceived as being in agreement with a similar line for the oleic acid-hexane system (Fig. 4). The plots of $\ln(J_{hex})$ and V_m/RT for both systems exhibit a linear relationship (Fig. 4), whereas some deviation of the relationship is detected for the triolein-hexane system ($R^2 = 0.91$) compared to the oleic acid-hexane system ($R^2 = 0.97$). The RS model can be applied when a change in the entropy of the mixing solvent with membrane polymer is ideal [23]. Therefore, the somewhat mismatching data for the triolein-hexane system (particularly with a greater concentration of triolein) may be due to a deviation from the ideal condition. This deviation is probably caused by entropy effects based on the molecular structure as discussed later, in Section 5.2.3

(2) Solvent flux

In the alcohol-hexane and the alkane-hexane systems, $\ln(J_s)$ can be linearly approximated by $V_m(\delta_{mem} - \delta_m)^2/RT$ or V_m/RT when the X values exceed 0.4 to 0.6, with a major deviation from the line for each system when the X values are less than 0.4 to 0.6 (Fig. 4). Hexane will swell the membrane remarkably, e.g., it was reported that the swelling of a PDMS dense membrane by pure hexane was about 200% [16]. Therefore, the major deviations may be due to a greater swelling of the membrane polymer due to the higher concentration of hexane as well as a lack of supplementation with the solvent on the feed-side.

In the lipid-hexane systems, a good linear relationship was found between $\ln(J_s)$ and V_m/RT based on the combined model (Fig. 4), similarly to the total and

hexane fluxes, while the data for undiluted triolein indicates significant deviation from the approximate line in the triolein-hexane system.

5.2.2 Analysis of approximately linear flux line with the combined model.

As mentioned above, the fluxes can be generalized by an approximated linear line as

$$J = \alpha \exp[-\beta (V_m (\delta_{mem} - \delta_m)^2/RT)] \text{ or, } \alpha \exp[-\beta (V_m/RT)] \qquad (22)$$

where α and β are the intercepts on the vertical axis and the slope (Fig. 4). This section discusses a physical meaning for "α" and "β" in this equation.

As a parallelism between Eq. (10) and Eq. (22), α and β correspond to (D ($\Delta p - \Delta\pi$)/λ^2) and Φ_{mem}^2, indicating that larger D and Δp and smaller $\Delta\pi$ and λ lead to larger α values, and moreover that a larger Φ_{mem} (i.e. a smaller swelling degree of the membrane) results in a larger β value. This concept is adopted with the total flux for each system appearing as α, β, reciprocal M_m (corresponding to the diffusivity), and mean *PR* values (Table 6). The *PR* value indicates the difference in the concentration of solvent between the feed side and permeation side. Therefore, *PR* is useful for guidance regarding the presence of osmotic pressure, as in the van 't Hoff law (Eq. (6)).

In the alcohol-hexane systems, α corresponds to the reciprocal of M_m (Table 6), indicating that the flux may be mainly dependent on the diffusivity by assuming a constant value of osmotic pressure for each system, whereas the β values are similar (Table 6), indicating that the mean degree of swelling is

constant.

In the alkane-hexane and diesel fuel-kerosene systems, $\Delta\pi$ can be assumed to be 0 because no concentration gradients through the membrane (the *PR* values) are observed (Table 6). The degree of swelling of the systems would be the same because of the similar β values (Table 6). The α value of the diesel fuel-kerosene system is somewhat higher than that of alkane-hexane system, despite the smaller reciprocal M_m (Table 6). This is presumably due to the wide distribution of the molecular weight for the diesel fuel-kerosene system and a slight difference in the membrane properties.

As a comparison of the oleic acid-hexane system with the alkane-hexane (or the diesel fuel-kerosene) system, the values of both α and β for the oleic acid-hexane system are larger than those of the other systems (Table 6). As a parallelism between the β value of the two systems, this could be regarded as a result of the greater degree of swelling of the membrane polymer for the alkane-hexane (or diesel fuel-kerosene) system. The difference in the α values may be explained as follows. The reciprocal value of M_m in the oleic acid-hexane system is less than in the alkane-hexane system (Table 6). Moreover, osmotic pressure will exist in the oleic acid-hexane system because of the positive value of *PR*, but not in the alkane-hexane (or diesel fuel-kerosene) system (Table 6). According to the combined model expressed as Eqs. (10) and (22), these data will lead to a smaller α value for the oleic acid-hexane system, but the result is in fact the opposite. This seeming conflict may be resolved by assuming that the greater degree of swelling of the membrane polymer as the alkane-hexane system will result in a larger value of λ, and that this larger λ value may exceed the effects of

the diffusivity and the osmotic pressure, resulting in a smaller α value for the alkane-hexane system.

From the above, in the present study, the linear relationships based on the combined model exhibit some contradictions and require some assumptions. For a more accurate analysis using this model, more detailed and exact determinations of values such as the degree of swelling, the diffusivity, and the osmotic pressure, as well as the permeate flux, are necessary.

5.3 Selectivity analysis using the combined model

Understanding the transport mechanism in organic solvent through a dense membrane requires characterizing the hexane-solvent-polymer interactions [27]. The *PR* values of alkane-hexane systems are almost 0, whereas the *PR* values of alcohol-hexane and lipid-hexane systems are positive (Table 4), in apparent correlation with a solution state of the binary system and membrane polymer, as indicated in the following discussion.

The thermodynamic criteria of solubility are based on the free energy of mixing, ΔG_{mix}[24]. When two substances are mutually soluble, ΔG_{mix} is defined by

$$\Delta G_{mix} = \Delta H_{mix} - T\,\Delta S_{mix} \tag{23}$$

where ΔH_{mix} is enthalpy mixing and ΔS_{mix} is entropy mixing.

In many cases, the mutual solution behavior of organic compounds such as the present binary solvent systems is governed by interactions and molecular

structures that mainly reflect the enthalpy and the entropy; a similarity of the two factors in an individual compound leads to higher mutual solubility [28]. A mutual solution, such as the present hexane dilution systems, can also be regarded from the standpoint of the RS model and can be expressed as

$$\ln a_s = \ln x_s + V_s \Phi_{hex}^2 (\delta_{hex} - \delta_s)^2 / RT, \quad (24)$$

where a_s is the activity of the solvent in the binary solution, x_s is the mole fraction of solvent in the binary solution, V_s is the molar volume of the solvent, δ_s is the solubility parameter of the solvent, Φ_{hex} is the volume fraction of hexane in the binary solution, and δ_{hex} is the solubility parameter of hexane in the binary solution. Here, $V_s (\delta_{hex} - \delta_s)^2$ is the coefficient of enthalpy mixing of solvent and hexane [23]. In the present study, we attempted to characterize the selectivity using the coefficient of enthalpy for solvent-hexane, solvent-membrane polymer, and hexane-membrane polymer.

In an alkane-hexane system, the mutual solution state is treated as "a perfect solution" because of its similar molecular structure and extremely low interaction [28]. The coefficient of enthalpy is 0.2 to 0.7 kJ/mol for solvent-hexane, 0.02 to 0.2 kJ/mol for a solvent-membrane polymer, and 0.05 kJ/mol for a hexane-membrane polymer. These very low values are similar (Table 7). The permeability through the membrane may behave as a single system (a pure solvent), in which case selectivity did not occur. In addition, the same behavior seems to occur in the diesel fuel-kerosene system, due to the unchanged composition of n-paraffin in the membrane process.

The pronounced difference in interaction forces as well as molecular structures seems to be nearly "an associated solution" [28]. In such a solution, preferential permeations of hexane occur. In alcohol-hexane systems, the coefficient of enthalpy for solvent-hexane (6.1 to 7.1 kJ/mol) and solvent-membrane polymer (5.1 to 6.4 kJ/mol) is much higher than that for hexane-membrane polymer (0.05 kJ/mol), corresponding to the positive mean *PR* value (Table 7). In lipid-hexane systems, the preferential permeations of hexane are remarkable, despite the fact that the coefficient of enthalpy for solvent-hexane (0.1 to 1.7 kJ/mol) and solvent-membrane (0.5 to 3.5 kJ/mol) is lower than that for the alcohol-hexane system (Table 7). This result may be a result of the major difference in the structure of solvent and hexane, corresponding to entropy mixing [28].

From the above discussion, when the entropy can de neglected owing to a similar structure of solvent and hexane, such as in alkane-hexane and alcohol-hexane systems, the selectivity of the solvent may be mainly determined by the coefficient of enthalpy for solvent-hexane and solvent-membrane polymer. Selectivity of the solvent may occur when major differences in the molecular structures of solvent and hexane are found, such as in a lipid-hexane system, even if the coefficient of enthalpy for solvent-hexane or solvent-membrane polymer is low.

6. Conclusions

The permeability of a PDMS-based dense membrane for binary solvent-hexane and diesel fuel-kerosene systems was analyzed using a model combining the regular solution model with the solution-diffusion model. Our main findings are

as follows.

·The combined model captures many important factors for analyzing the transport mechanism, such as the diffusivity, degree of swelling of the membrane polymer, membrane thickness, and osmotic pressure.

·The time courses of total flux for all systems indicate a pseudo-static condition of solvents, hexane, and membrane polymer; therefore, it was reasonable to analyze the transport mechanism using the combined model.

·The solution-diffusion model can be applied to the total and hexane fluxes, where the solubility corresponds to the solubility parameter difference between membrane polymer and solvent ($|\delta_{mem} - \delta_s|$), and the diffusivity corresponds to the molecular weight of solvents, though some limitations were found.

·The combined model was applied to analyze the transport mechanism for the present systems. The mean molar total flux $\ln(J_T)$ and hexane flux $\ln(J_{hex})$ exhibited a linear dependency on the product of the mean molar volume of solvent and hexane (V_m) and the square of the solubility parameter difference between the membrane polymer and solvent-hexane $(\delta_{mem} - \delta_m)^2$ at constant pressure and temperature. $\ln(J_T)$ and $\ln(J_{hex})$ for the alcohol-hexane systems decreased linearly with an increase in $V_m(\delta_{mem} - \delta_m)^2/RT$; however, $\ln(J_T)$ and $\ln(J_{hex})$ for the alkane-hexane, fuel-kerosene, and lipid-hexane systems, except for the data for undiluted triolein, decreased only with an increase in V_m/RT, due to the fact that the $(\delta_{mem} - \delta_m)$ values were numerically around unity.

·In the lipid-hexane systems, an approximately linear relationship existed between the solvent flux $\ln(J_s)$ and V_m/RT, while in the alcohol-hexane and alkane-hexane systems, linear relationships between $\ln(J_s)$ and $V_m(\delta_{mem} -$

$\delta_m)^2/RT$ *or* V_m/RT were found when the weight fraction of solvent in the feed X exceeded 0.4 to 0.6.

·Unchanged compositions of permeate were observed for the alkane-hexane and diesel-fuel-kerosene systems, while preferential permeations of hexane were observed in the alcohol-hexane and lipid-hexane systems. The selectivity of the solvent may be determined by the similarity of structure between hexane and solvent and by the solvent-hexane-membrane polymer interaction.

References

[1] R. W. Baker, N. Yoshioka, J. M. Mohr, A. J. Khan, Separation of organic vapors from air, J. Membr. Sci. 31 (1987) 259-271.

[2] A. Ito, K. Adachi, Y. Feng, Separation of Aromatics by vapor permeation through solvent swollen membrane, J. Chem. Eng. Japan. 28 (1995) 679-683.

[3] Li. Liu, N. Jiang, C. M. Burns, X. Feng, Substrate resistance in composite membranes for organic vapour/gas separations, J. Membr. Sci. 338 (2009) 153-160.

[4] T. Yamaguchi, S. Nakao, S. Kimura, Design of pervaporation membrane for organic-liquid separation based on solubility control by plasma-graft filling polymerization technique, Ind. Eng. Chem. Res. 32 (1993) 848-853.

[5] J. Chen, J. Li, R. Qi, H. Ye, C. Chen, Pervaporation performance of crosslinked polydimethylsiloxane membranes for deep desulfurization of FCC gasoline, I. Effect of different sulfur species, J. Membr. Sci. 322 (2008) 113-121.

[6] J. P. Robinson, E. S. Tarleton, C. R. Millington, A. Nijmeijer, Solvent flux through dense polymeric nanofiltration membranes, J. Membr. Sci. 230 (2004) 29-37.

[7] E. S. Tarleton, J. P. Robinson, S. J. Smith, J. J. W. Na, New experimental measurements of solvent induced swelling in nanofiltration membranes, J. Membr. Sci. 261 (2005) 129-135.

[8] R. Subramanian, M. Nakajima, K.S.M.S. Raghavarao, T. Kimura, Processing vegetable oils using nonporous denser polymeric composite membranes, J. Am. Oil Chem. Soc. 81 (2004) 313-322.

[9] S. Manjula, R. Subramanian, Membrane technology in degumming, dewaxing, deacidifying and decolorizing edible oils, Crit. Rev. Food Sci. Nutr. 46 (2006) 569-592.

[10] A. Miyagi, M. Nakajima, H. Nabetani, R. Subramanian, Feasibility of recycling used frying oil using membrane process, Eur. J. Lipid Sci. Technol. 103 (2001) 208-215.

[11] A. Miyagi, R. Subramanian, M. Nakajima, Membrane and additional adsorption processes for quality improvement of used frying oil, J. Am. Oil Chem. Soc. 80 (2003) 927-932.

[12] A. Miyagi, H. Nabetani, M. Nakajima, Reduction in oxidation index value of fish oils using hydrophobic nonporous denser membrane process, Food Sci. Tech. Res. 15 (2009) 245-248.

[13] A. Miyagi, H. Nabetani, R. Subramanian, Purification of crude fatty acids using a PDMS-based composite membrane, Sep. Purif. Technol. 77 (2011) 80-86.

[14] J. G. Wijimans, R.W. Baker, The solution-diffusion model: a review, J. Membr. Sci. 163 (1995) 1-21.

[15] Machado, D. R., D. Hasson and R. Semiat; Effect of solvent properties on permeate flow through nanofiltration membranes. part I: investigation of parameters affecting solvent flux, J. Membr. Sci. 163 (1999) 93-102

[16] N. Stafie, D. F. Stamatialis, M. Wessling, Insight into the transport of hexane-solute systems through tailor-made composite membranes, J. Membr. Sci. 228 (2004) 103-116.

[17] S. J. Han, S. S. Luthra, L. Peeva, X. J. Yang, A. G. Livingston, Insights into the transport of toluene and phenol through organic solvent nanofiltration membranes, Sep. Sci. Technol. 38 (2003) 1899-1923.

[18] R. Subramanian, K.S.M.S. Raghavarao, H. Nabetani, M. Nakajima, T. Kimura, T. Maekawa, Differential permeation of oil constituents in nonporous denser polymeric membranes, J. Membr Sci. 187 (2001) 57-69.

[19] R. Subramanian, K. S. M. S. Raghavarao, M. Nakajima, H. Nabetani, T. Yamaguchi, T. Kimura, Application of dense membrane theory for differential permeation of vegetable oil constituents, J. Food Eng. 60 (2003) 249-256.

[20] S. Manjula, H. Nabetani, R. Subramanian, Flux behavior in a hydrophobic dense membrane with undiluted and hexane-diluted vegetable oils, J. Membr. Sci. 366 (2011) 43-47.

[21] A. Miyagi, M. Murata, H. Nabetani, M. Nakajima, R. Subramanian, Analysis of permeability of organic solvents through a composite dense nonporous membrane, J. Chem. Eng. Japan. 43 (2010) 261-268.

[22] D. Hofmann, L. Fritz, J. Ulbrich, C. Schepers, M. Bohning, Detailed-atominic molecular modeling of small molecule diffusion and solution processes in polymeric membrane materials, Macromol. Theory Simul. 9 (2000) 293-327

[23] K. Shinoda, Principles of solution and solubility, Marcel Dekker, New York, (1978) pp. 55-73, 123-156, 200-211.

[24] D. W. V. Krevelen, Cohesive properties and solubility, Properties of polymers, 4th edn., Elsevier, Amsterdam, (2008) pp.189-227.

[25] S. Yoshikawa, Use of solvents (Youzainoriyou), The handbook of solvents (Youzai-handbook), edited by S, Asahara, J. Tokura, S. Oogawara, J. Kumanoya and M. Aneo, Koudan Corp., Tokyo, (1985) p.92. (in Japanese)

[26] R. F. Fedors, A method for estimating both the solubility parameters and molar volumes of liquids, Polym. Eng. Sci. 14 (1974) 147-154.

[27] X. J. Yang, A. G. Livingston, L. F. D. Santos, Experimental observations of nanofiltration with organic solvents, J. Membr. Sci. 190 (2001) 45-55.

[28] M. Aneo, Phenomenon of dissolution (Youkaigensyo), The handbook of solvents (Youzai-handbook), edited by S, Asahara, J. Tokura, S. Oogawara, J. Kumanoya and M. Aneo, Koudan Corp., Tokyo, (1985) pp.1-12. (in Japanese)

Nomenclature

A	= effective membrane area (0.0032 m^2)
a	= activity of solvent in membrane phase [-]
a_s	= activity of solvent in binary solution [-]
C_f	= penetrant concentration of feed-side [kg/m^3]
C_p	= penetrant concentration of permeation-side [kg/m^3]
D	= diffusion coefficient [m^2/h]
dC/dz	= concentration gradient [$(kg/m^3)/m$]
$d\mu/dz$	= gradient in chemical potential [N/mol]
E_{coh}	= internal energy of structural group [J/mol]
J	= permeate flux [$kg/(m^2\ h)$]
J_{hex}	= hexane flux [$kg/(m^2\ h)$]
J_s	= solvent flux [$kg/(m^2\ h)$]
J_T	= total flux [$kg/(m^2\ h)$]
J_0	= initial total flux [$kg/(m^2\ h)$]
J_{30}	= total flux when the total amount of permeate reached 30 g [$kg/(m^2\ h)$]
L	= coefficient of proportionality linking chemical potential [$(mol\ h)/m^3$]
M	= molecular weight [g/mol]
M_m	= mean molecular weight [g/mol]
M_i	= molecular weight of component *i* [g/mol]
PD	= percentage decrease of total flux [%]
PR	= percentage rejection of solvent [%]
p_f	= pressure of feed-side [Pa] or [kgf/m^2]
p_p	= pressure of permeation-side [Pa] or [kgf/m^2]
R	= gas constant [J/(mol K)]
S	= solubility coefficient [m^{-1}]
T	= absolute temperature [K]
t	= permeation time [h]
V	= molar volume [cm^3/mol]
V_{hex}	= molar volume of hexane [cm^3/mol]
V_g	= molar volume of structural group [cm^3/mol]

V_m = mean molar volume [cm^3/mol]

V_i = molar volume of component *i* [cm^3/mol]

V_s = molar volume of solvent [cm^3/mol]

W = amount of permeate [kg]

X = weight fraction of solvent in feed [-]

x = mole fraction of solvent in membrane polymer phase [-]

x_s = mole fraction of solvent in binary solution [-]

x' = mole fraction of solvent in solvent (feed) phase [-]

Y = weight fraction of solvent in permeate [-]

y_i = mole fraction of component *i* [-]

α = intercept value of a vertical axis in Fig. 4

β = slope value in Fig. 4

ΔC = difference in concentration [mol/L] or [kg/m^3]

Δp = difference in pressure [Pa] or [kgf/m^2]

ΔH = heat of vaporization [J/mol]

ΔG_{mix} = free energy of mixing [J/mol]

ΔH_{mix} = enthalpy mixing [J/mol]

ΔS_{mix} = entropy mixing [J/(mol K)]

$\Delta \pi$ = osmotic pressure [Pa] or [kgf/m^2]

δ = solubility parameter [J/cm^3]$^{1/2}$

δ_d = solubility parameter of dispersion forces [J/cm^3]$^{1/2}$

δ_h = solubility parameter of hydrogen bonding [J/cm^3]$^{1/2}$

δ_{hex} = solubility parameter of hexane [J/cm^3]$^{1/2}$

δ_i = solubility parameter of component *i* [J/cm^3]$^{1/2}$

δ_m = mean solubility parameter of solvent-hexane [J/cm^3]$^{1/2}$

δ_{mem} = solubility parameter of membrane polymer (PDMS) [J/cm^3]$^{1/2}$

$\delta_{n\text{-}p}$ = solubility parameter of n-paraffin [J/cm^3]$^{1/2}$

δ_p = solubility parameter of dipole-dipole interaction [J/cm^3]$^{1/2}$

δ_s = solubility parameter of solvent [J/cm^3]$^{1/2}$

Φ_{hex} = volume fraction of hexane in binary solution [-]

Φ_{mem}	= volume fraction of membrane polymer in membrane phase [-]
Φ'_{mem}	= volume fraction of membrane polymer in retentate [-]
λ	= membrane thickness [m]
μ	= chemical potential [J/mol]

Table 1. Properties of membrane polymer and organic solvents[a]

Description	V [cm^3/mol]	M [g/mol]	δ [$(J/cm^3)^{1/2}$]	$\lvert \delta_{mem} - \delta_s \rvert$ [$(J/cm^3)^{1/2}$]
Membrane polymer				
Polydimethylsiloxane (PDMS)	-	-	15.5[b]	-
Solvents				
Ethanol	58	46	26.0[b]	10.5
1-Butanol	92	74	23.3[b]	7.8
1-Hexanol	125	102	21.9[b]	6.4
Hexane	132	86	14.9[c]	0.6
Decane	196	142	15.8[c]	0.3
Tridecane	245	184	16.2[c]	0.7
Hexadecane	294	226	16.4[c]	0.9
Oleic acids	317	283	14.3[d]	1.2
Trioleine	983	885	13.6[d]	1.9

[a] V, molar volume; δ, solubility parameter (25°C); δ_{mem}, solubility parameter of PDMS; δ_s, solubility parameter of solvent.

[b] Ref. [21]

[c] calculated; $\delta = (\Sigma E_{coh} / \Sigma V_g)^{1/2}$: Ref [26]

[d] Ref. [13]

Table 2. Operating conditions of gas chromatography

Binary system	Ethanol-hexane	1-Butanol-hexane	1-Hexanol-hexane	Decane-hexane	Tridecane-hexane	Hexadecane-hexane	Diesel Fuel-kerosene
Column	Gaskuropack 54 60/80 (GL Sciences Corp.) Glass I.D.3ϕ × 2 m	PEG-20M, 15% Uniport HP, 60/80 (GL Sciences Corp.) Glass I.D.3ϕ × 2 m	Gaskuropack 54 60/80 (GL Sciences Corp.) Glass I.D.3ϕ × 2 m	Silicone SE-30, 20% Uniport B, 60/80 (GL Sciences Corp.) Glass I.D.3ϕ × 2 m	Silicone SE-30, 20% Uniport B, 60/80 (GL Sciences Corp.) Glass I.D.3ϕ × 2 m	Silicone SE-30, 20% Uniport B, 60/80 (GL Sciences Corp.) Glass I.D.3ϕ × 2 m	Silicone SE-30, 20% Uniport B, 60/80 (GL Sciences Corp.) Glass I.D.3ϕ × 2 m
Carrier gas (Flow rate)	N_2 (50 mL/min)	N_2 (30 mL/min)	N_2 (75 mL/min)	N_2 (40 mL/min)	N_2 (50 mL/min)	N_2 (40 mL/min)	N_2 (40 mL/min)
Column temp. or Programmed temp.	200°C	120°C	230°C	Initial temp., 40°C (Hold, 2 min) Rate, 20°C/min Final temp, 150°C (Hold, 10 min)	Initial temp., 40°C (Hold, 2 min) Rate, 20°C/min Final temp, 230°C (Hold, 10 min)	Initial temp., 40°C (Hold, 2 min) Rate, 20°C/min Final temp, 270°C (Hold, 10 min)	Initial temp., 50°C (Hold, 0 min) Rate, 10°C/min Final temp, 280°C (Hold, 20 min)
Injection temp.	230°C	160°C	250°C	200°C	250°C	270°C	300°C
Detector (Temp.)	FID (230°C)	FID (170°C)	FID (250°C)	FID (200°C)	FID (250°C)	FID (270°C)	FID (300°C)

Table 3. Group contributions of E_{coh} and V_g[a] [24]

Group	E_{coh} [J/mol]	V_g [cm^3/mol]
$-CH_3$	4710	33.5
$-CH_2-$	4940	16.1

[a] E_{coh}, internal energy; V_g, internal molar volume

Table 4. X, Y, M_m, V_m, $|\delta_{mem}-\delta_m|$, J_T, J_{hex}, J_s and PR values of solvent-hexane system (25°C, 1 MPa)[a]

X [kg/kg]	Y [kg/kg]	M_m [g/mol]	V_m [cm^3/mol]	$\lvert\delta_{mem}-\delta_m\rvert$ [$(J/cm^3)^{1/2}$]	J_T [kg/(m^2 h)]	J_{hex} [kg/(m^2 h)]	J_s [kg/(m^2 h)]	PR [%]
Alcohol-hexane system								
Ethanol-hexane								
0	0	86	132	0.6	71.2	71.2	0	-
0.202	0.141	80	115	0.7	59.2	50.9	8.3	30
0.399	0.259	76	103	1.8	32.0	23.7	8.3	35
0.602	0.492	66	84	4.2	15.8	8.0	7.8	18
0.802	0.766	55	68	7.5	7.2	1.7	5.5	4
1	1	46	58	10.5	2.1	0	2.1	-
1-Butanol-hexane								
0	0	86	132	0.6	73.6	73.6	0	-
0.209	0.161	84	125	0.5	49.8	41.7	8.0	23
0.402	0.335	82	117	1.8	34.3	22.8	11.5	17
0.600	0.531	80	109	3.4	19.3	9.1	10.3	11
0.796	0.748	77	101	5.3	10.3	2.6	7.7	6
1	1	74	92	7.8	4.0	0	4.0	-
1-Hexanol-hexane								
0	0	86	132	0.6	75.3	75.3	0	-
0.200	0.146	88	131	0.2	41.7	35.6	6.1	27
0.397	0.328	91	130	1.4	28.1	18.9	9.2	18
0.598	0.570	95	128	3.0	15.8	6.8	9.0	5
0.800	0.776	98	127	4.5	8.2	1.8	6.4	3
1	1	102	125	6.4	3.7	0	3.7	-
Alkane-hexane system								
Decane-hexane								
0	0	86	132	0.6	78.8	78.8	0	-
0.194	0.181	96	140	0.5	72.3	59.2	13.1	7
0.402	0.382	107	149	0.3	59.1	36.5	22.6	5
0.596	0.605	120	163	0.1	50.4	19.9	30.5	-2
0.786	0.786	130	176	0.1	39.0	8.3	30.7	0
1	1	142	196	0.3	29.6	0	29.6	-
Tridecane-hexane								
0	0	86	132	0.6	79.2	79.2	0	-
0.221	0.228	108	146	0.3	68.9	53.2	15.7	-3
0.398	0.394	125	158	0.1	52.1	31.6	20.5	1
0.598	0.598	145	178	0.2	40.3	16.2	24.1	0
0.770	0.771	162	201	0.5	28.6	6.5	22.1	0
1	1	184	245	0.9	16.4	0	16.4	-
Hexadecane-hexane								
0	0	86	132	0.6	78.8	78.8	0	-
0.194	0.202	114	146	0.1	65.3	52.1	13.2	-4
0.392	0.384	140	163	0.3	50.0	30.8	19.2	2
0.614	0.615	172	193	0.6	32.4	12.5	19.9	0
0.809	0.812	200	233	0.8	20.3	3.8	16.5	0
1	1	226	294	0.9	8.5	0	8.5	-
Lipid-hexane system								
Oleic acids-hexane								
0	0	86	132	0.6	74.1	74.1	0	-
0.214	0.131	112	156	0.7	49.3	42.8	6.5	39
0.408	0.370	159	200	0.8	15.6	9.8	5.8	9
0.594	0.565	197	237	0.9	8.4	3.7	4.7	5
0.801	0.768	237	274	1.0	3.7	0.9	2.8	4
1	1	283	317	1.2	0.7	0	0.7	-
Trioleine-hexane								
0	0	86	132	0.6	74.1	74.1	0	-
0.212	0.106	171	222	0.7	21.5	19.2	2.3	50
0.412	0.239	277	335	0.8	11.6	8.8	2.8	42
0.602	0.516	498	571	1.2	3.8	1.8	2.0	14
0.807	0.749	684	769	1.5	0.9	0.2	0.7	7
1	1	885	983	1.9	0.1	0	0.1	-

[a] X, weight fraction of solvent in feed; Y, weight fraction of solvent in permeate; M_m, mean molecular weight of permeate; V_m, mean molar volume of permeate; $|\delta_{mem}-\delta_m|$, difference of mean solubility parameter of membrane and solvent-hexane in permeate; J_T, total flux; J_{hex}, hexane flux; J_s, solvent flux; PR, percentage rejection.

Table 5. Compositions of n-paraffin of feed and permeate, and M_m, V_m, J_T, $\delta_{n\text{-}p}$ and $|\delta_{mem}\text{-}\delta_{n\text{-}p}|$ values of diesel fuel-kerosene system (25°C, 1 MPa)[a]

n-paraffin composition	Kerosene		Diesel fuel-kerosene, 20/80		Diesel fuel-kerosene, 40/60		Diesel fuel-kerosene, 60/40		Diesel fuel-kerosene, 80/20		Diesel fuel		$\delta_{n\text{-}p}$[b]	$\lvert\delta_{mem}-\delta_{n\text{-}p}\rvert$
[%]	Feed	Permeate	Feed	Permeate	Feed	Permeate	Feed	Permeate	Feed	Permeate	Feed	Permeate	$[(J/cm^3)^{1/2}]$	$[(J/cm^3)^{1/2}]$
C 8	3.5	3.6	2.8	2.9	2.2	2.3	1.7	1.7	1.2	1.2	0.7	0.7	15.5	0.0
C 9	17.7	18.0	14.2	13.8	10.9	11.5	7.1	8.5	4.9	5.0	2.6	2.7	15.6	0.1
C10	15.2	15.5	12.4	12.6	9.6	10.0	7.4	7.5	5.1	5.2	2.2	2.8	15.8	0.3
C11	16.5	16.6	13.4	13.7	10.8	11.3	8.5	8.7	6.2	6.4	2.6	3.0	15.9	0.4
C12	15.2	15.1	12.7	12.8	10.5	10.7	8.7	8.7	6.7	6.9	2.7	2.9	16.1	0.6
C13	11.9	11.7	10.2	10.3	8.9	8.9	7.5	7.6	6.3	7.0	5.3	3.1	16.2	0.7
C14	11.5	11.1	10.8	10.8	10.4	10.3	9.9	9.9	9.3	9.4	9.0	9.3	16.2	0.7
C15	6.2	6.2	6.7	6.6	7.4	7.3	8.0	8.2	8.5	9.3	9.5	10.2	16.3	0.8
C16	1.8	1.9	4.1	4.1	6.0	5.9	7.7	7.8	9.3	9.3	11.4	12.1	16.4	0.9
C17	0.4	0.4	2.8	2.8	5.0	4.9	7.1	6.9	8.9	8.7	11.2	11.5	16.5	1.0
C18	0.1	0.0	2.4	2.3	4.4	4.1	6.2	5.9	7.8	7.6	10.1	10.2	16.5	1.0
C19	0.1	0.0	1.8	1.8	3.4	3.2	5.0	4.7	6.2	6.0	7.9	7.9	16.6	1.1
C20	0.0	0.0	1.5	1.4	2.8	2.6	4.0	3.8	5.1	4.7	6.3	6.3	16.6	1.1
C21	0.0	0.0	1.2	1.2	2.2	2.0	3.2	2.8	4.0	3.7	5.1	5.0	16.6	1.1
C22	0.0	0.0	0.9	0.9	1.7	1.5	2.5	2.2	3.1	2.8	3.9	3.7	16.7	1.2
C23	0.0	0.0	1.1	1.0	1.9	1.7	2.8	2.5	3.6	3.2	4.5	4.2	16.7	1.2
C24	0.0	0.0	0.7	0.6	1.2	1.0	1.7	1.5	2.2	2.0	2.8	2.6	16.7	1.2
C25	0.0	0.0	0.3	0.3	0.6	0.5	0.9	0.7	1.1	1.0	1.4	1.3	16.8	1.3
C26	0.0	0.0	0.1	0.1	0.2	0.2	0.3	0.2	0.4	0.4	0.6	0.5	16.8	1.3
M_m [g/mol]	158		170		180		192		206		226			
V_m [cm^3/mol]	213		227		239		254		270		293			
J_T [kg/(m^2 h)]	32.4		26.1		19.5		15.8		12.7		8.9			

[a] $\delta_{n\text{-}p}$, solubility parameter of n-paraffin; for other abbreviations see Tables 1and 4.

[b] calculated; $\delta = (\Sigma E_{coh}/\Sigma V_g)^{1/2}$: Ref [26].

Table 6. α and β, reciprocal of $M_{m,}$ and mean of PR (for total flux)[a]

Binary system	α	β	Reciprocal of M_m [mmol/g]	Mean of PR [%]
Alcohol-hexane				
Ethanol-hexane	44	1.2	15.5	22
Butanol-hexane	41	1.1	12.4	14
Hexanol-hexane	32	1.1	10.7	13
Alkane-hexane	620	39	7.7	0
Diesel fuel-kerosene	1000	40	5.3	0[b]
Oleic acid-hexane	1200	61	6.6	14

[a] α, the intercepts on the vertical axis in Fig. 4; β, the slope in Fig. 4; for other abbreviations see Table 4.

[b] PR is regarded as 0 because there is no change in n-paraffin composition.

Table 7. Relationships between mean of *PR* and coefficients of enthalpy of solvent-hexane, solvent-membrane polymer and hexane-membrane polymer[a]

Binary systems	$V_s(\delta_{hex}-\delta_s)^2$ [kJ/mol]	$V_s(\delta_{mem}-\delta_s)^2$ [kJ/mol]	$V_{hex}(\delta_{mem}-\delta_{hex})^2$ [kJ/mol]	Mean of *PR* [%]
Alcohol-hexane system				
Ethanol-hexane	7.1	6.4	0.05	22
1-Butanol-hexane	6.5	5.6	0.05	14
1-Hexanol-hexane	6.1	5.1	0.05	13
Alkane-hexane system				
Decane-hexane	0.2	0.02	0.05	2
Tridecane-hexane	0.4	0.1	0.05	-1
Hexadecane-hexane	0.7	0.2	0.05	-1
Lipid-hexane				
Oleic acids-hexane	0.1	0.5	0.05	14
Trioleine-hexane	1.7	3.5	0.05	28

[a] $V_s(\delta_{hex}-\delta_s)^2$, $V_s(\delta_{mem}-\delta_s)^2$ and $V_{hex}(\delta_{mem}-\delta_{hex})^2$, coefficients of enthalpy of solvent-hexane, solvent-membrane polymer and hexane-membrane polymer, respectively; for other abbreviations see Table 4.

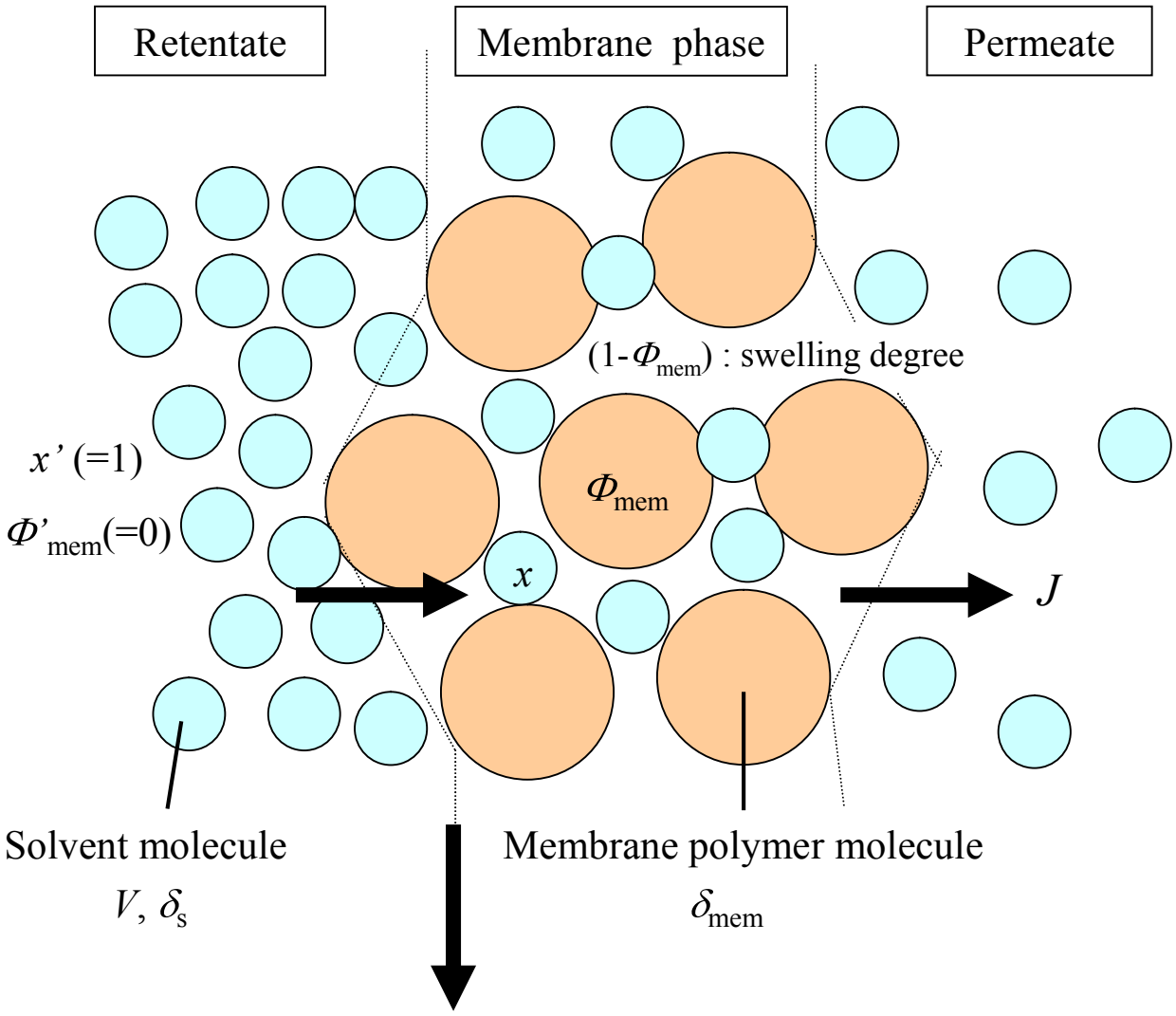

Equilibrium on the interface of the membrane polymer

$$\ln x + V \Phi_{mem}^{2} (\delta_{mem} - \delta_s)^2/RT = \ln x' + V\Phi'^{2}_{mem} (\delta_{mem} - \delta_s)^2/RT$$

Fig. 1

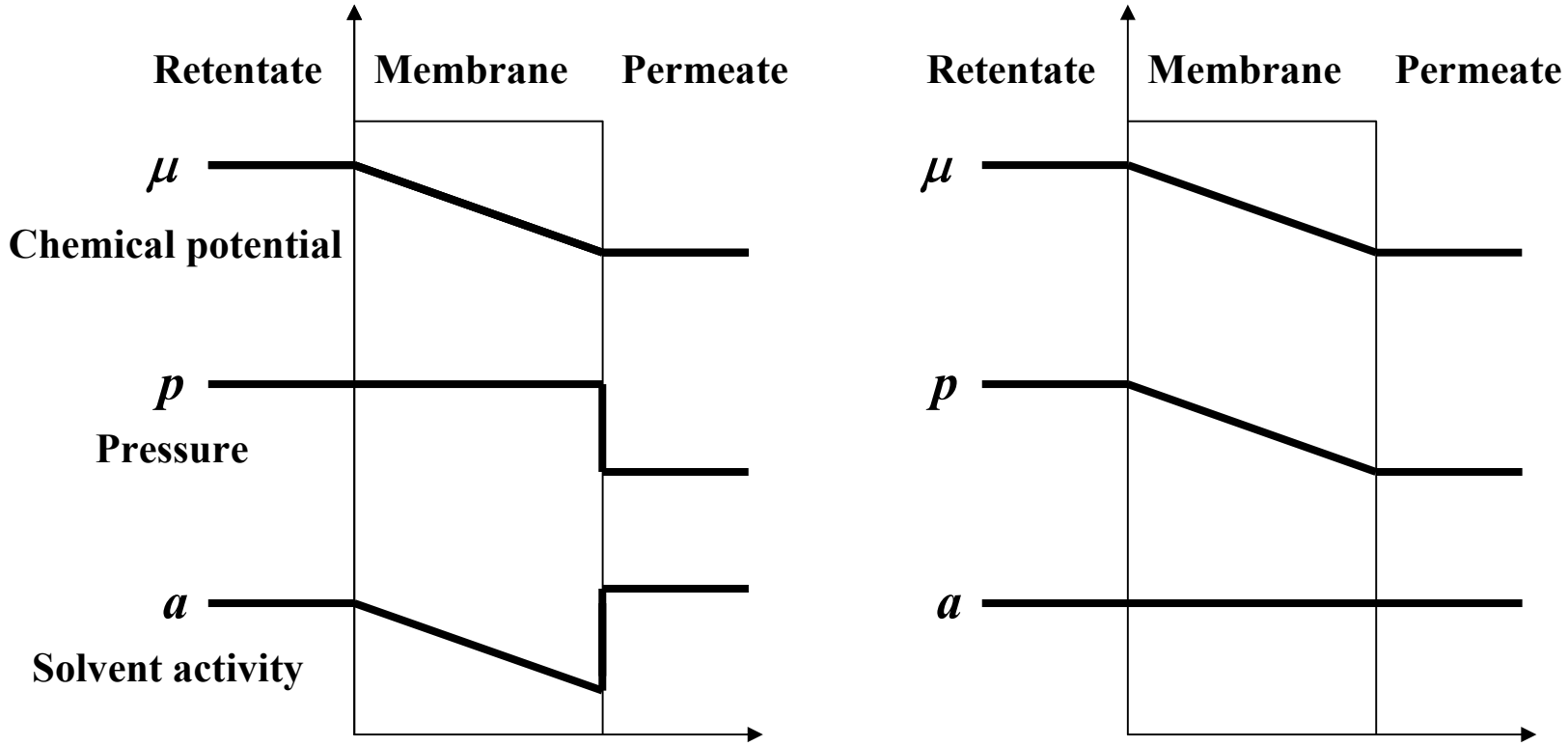
(a) Solution-diffusion model: [14]
(b) Regular solution model
Retentate
Membrane
Permeate
μ
Chemical potential
p
Pressure
a
Solvent activity
Retentate
Membrane
Permeate
μ
p
a

Fig. 2

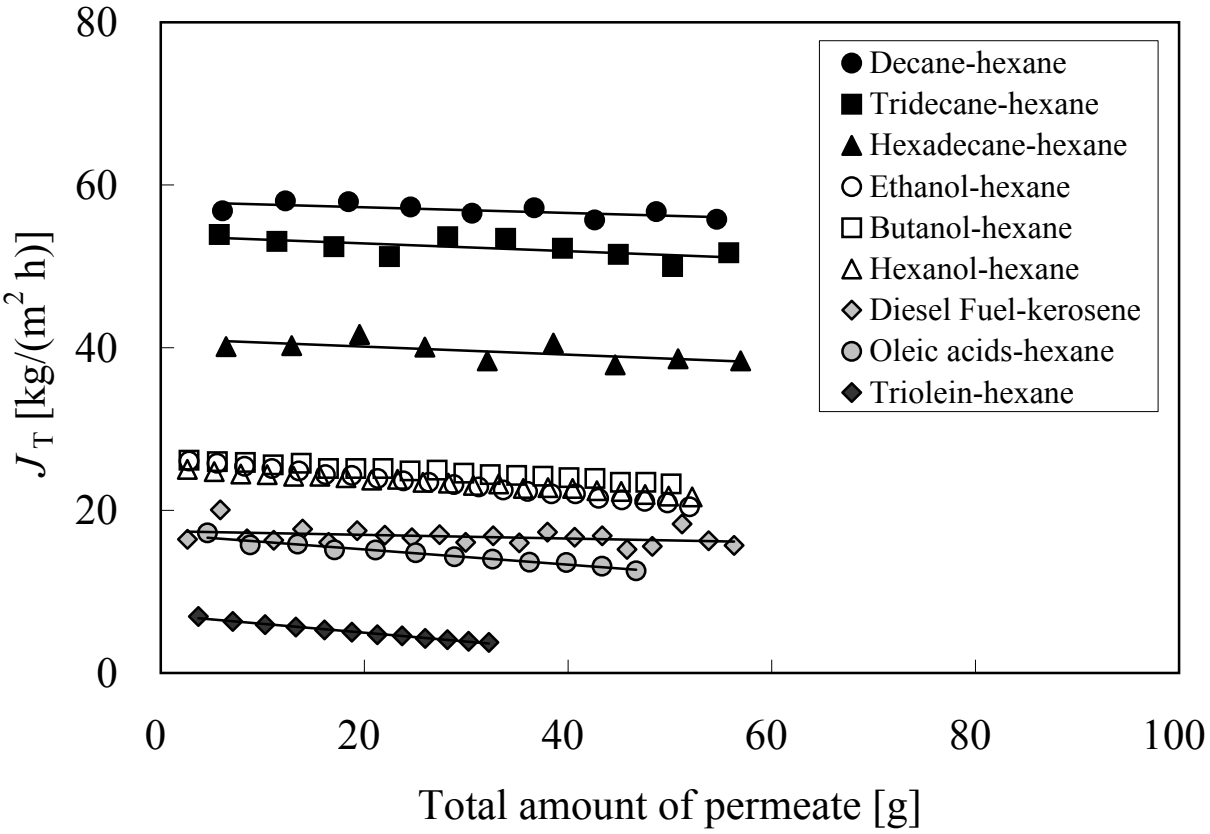
80
60
40
20
0
J_T [kg/(m^2 h)]
0
20
40
60
80
100
Total amount of permeate [g]
Decane-hexane
Tridecane-hexane
Hexadecane-hexane
Ethanol-hexane
Butanol-hexane
Hexanol-hexane
Diesel Fuel-kerosene
Oleic acids-hexane
Triolein-hexane

Fig.3

(a) Alcohol-hexane system

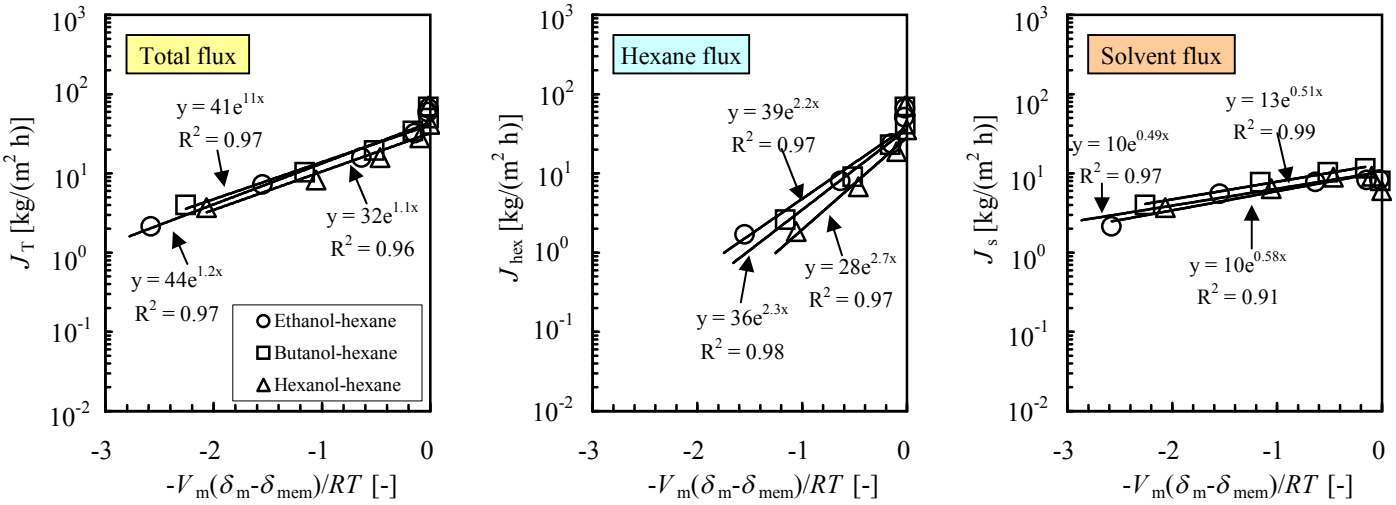

(b) Alkane-hexane, and diesel fuel-kerosene systems

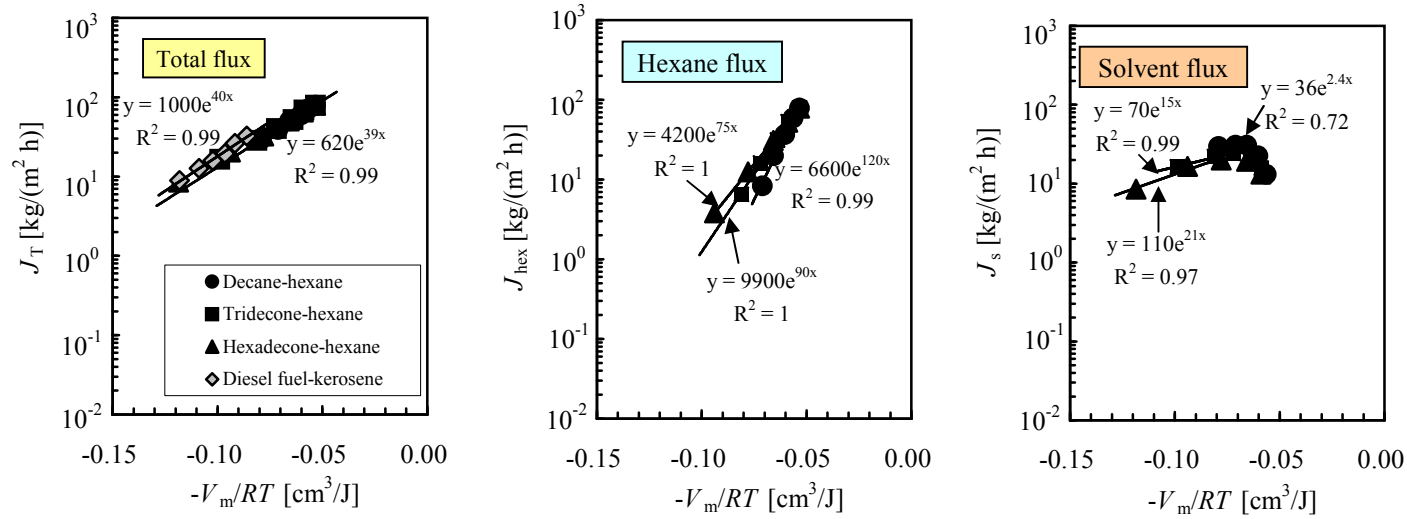

(c) Lipid-hexane system

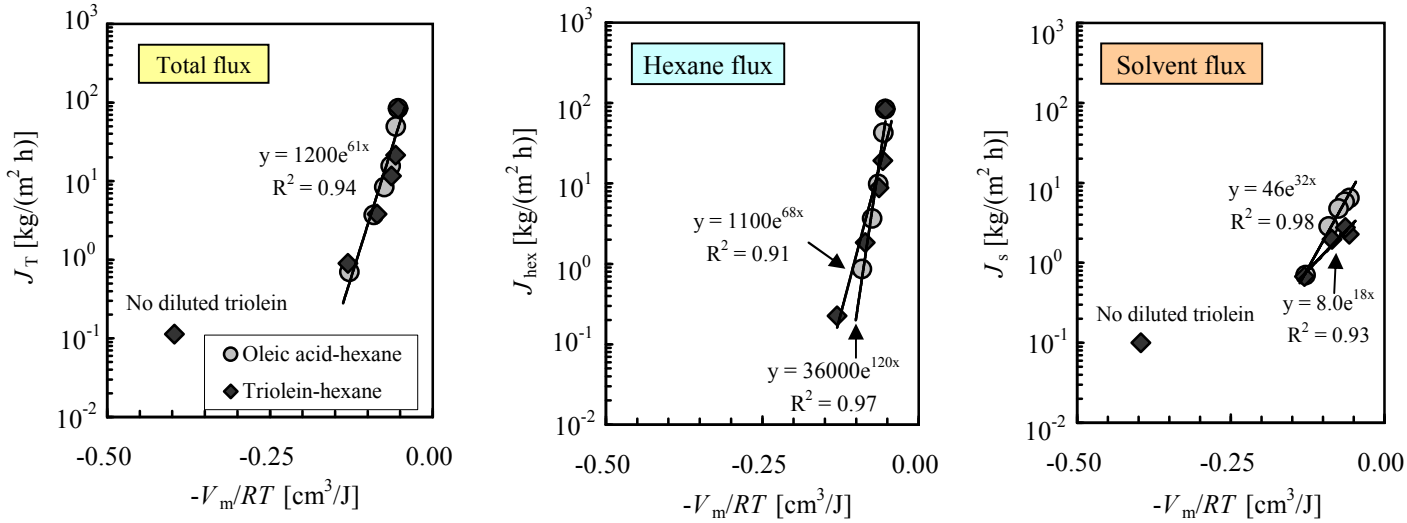

Fig. 4

Figure captions

Fig. 1. Scheme of a pseudo-static solution of solvent in the membrane polymer in equilibrium with the solvent phase (retentate) based on the regular solution model.

Fig. 2. Profiles of chemical potential, pressure, and activity (concentration) across the membrane according to the solution-diffusion model and the regular solution model.

Fig 3. Total permeate flux *vs.* total amount of permeate (initial charging: 100 g of 50/50 [g/g] solvent-hexane and diesel fuel-kerosene, at 25^{o}C, 1 MPa).

Fig. 4. Permeate flux ($\ln(J_T)$, $\ln(J_{hex})$ and $\ln(J_s)$) *vs.* $-V_m(\delta_m - \delta_{mem})^2/RT$ or $-V_m/RT$ (25^{o}C, 1 MPa).